Title Here

Author 1, Author 2

Author Affiliation

Introduction

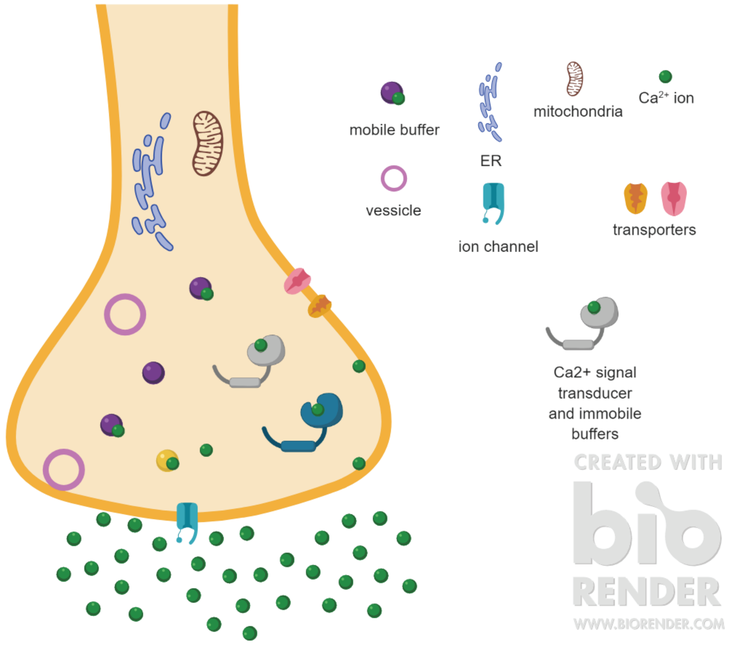

Ca^{2+} triggers the release of transmitters from nerve terminals and hormones from endocrine cells. Ca^{2+} signals initiated by Ca^{2+} entry through voltage-gated channels are shaped by Ca^{2+} binding to cytosolic buffers. While the channels have been well characterized, less is known about the buffers. These proteins rapidly bind 97.5-99.5% of Ca^{2+} ions upon entry. Ca^{2+} sources, sinks, and buffers form a highly regulated but very dynamic system. The complex interaction between transport and binding presents a formidable challenge to the quantitative study of cellular Ca^{2+} signaling. Buffers limit the rise in Ca^{2+}, set up steep gradients around sites of entry, control Ca^{2+} diffusion, limit the rate of Ca^{2+} extrusion and sequestration, and determine the availability of Ca^{2+} for downstream signaling targets. The molecular structures of many buffers are known and their Ca^{2+} binding properties have been well studied in vitro. However, their concentrations, binding properties, and mobility are different in a cellular context. We have used fluorescence imaging in posterior pituitary nerve terminals to explore cytosolic Ca^{2+} buffers in situ. Previous work in pituitary terminals identified two Ca2+ buffers, determined their Kd and concentration, and estimated their mobility. Western blots revealed the well-known cytosolic Ca2+ buffers calretinin and calbindin D28K, and their Kd's are consistent with our measurements. Here we present preliminary work investigating the effective (or apparent) diffusion coefficient (D_{app}) of Ca^{2+} in whole cell patch clamped nerve terminals.

Methods

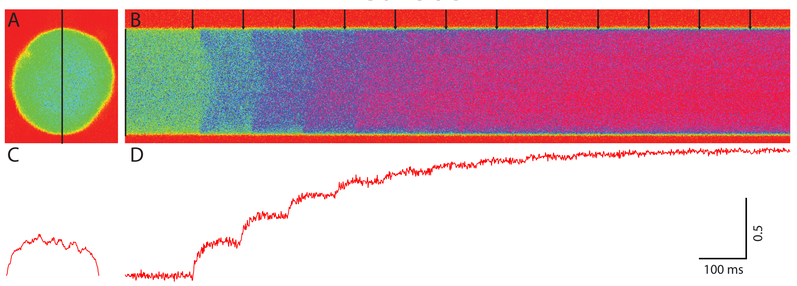

Fig 1. A. A nerve terminal in the posterior pituitary is patched, introducing 50 μM Cal-520 into the cytosol. B. Fluorescence vs y (vertical axis) and t (horizontal axis) is acquired by scanning the excitation laser along the indicated line. A sequence of voltage steps from -80 mV to +10 mV is delivered at 10 Hz (black arrows). C. Fluorescence vs y before the first stimulus reveals a standing gradient. D. Fluorescence vs time shows initially robust changes in fluorescence with amplitude decreasing during stimulus train duration.

$[Ca^{2+}]_{Free}$ is calculated from fluorescence using eq. 1. Rearranging Fick's law gives the diffusion constant, eq. 2. Near the center of a spherical nerve terminal, eq. 2 simplifies to eq. 3. Buffered Ca2+ diffusion is described in eq. 4.

$$1.)\quad [Ca^{2+}] = K_D \frac{F - {}^{1}/_{R_f}}{1 - F} \qquad 2.)\quad D_{app} = \frac{\frac{\partial [Ca^{2+}]}{\partial t}}{\left(\frac{\partial^2 [Ca^{2+}]}{\partial x^2} + \frac{\partial^2 [Ca^{2+}]}{\partial y^2} + \frac{\partial^2 [Ca^{2+}]}{\partial z^2}\right)} \qquad 3.)\quad D_{app} \cong \frac{\frac{\partial F}{\partial t}}{3\frac{\partial^2 F}{\partial x^2}}$$

$$4.)\quad D_{app} = \frac{[Ca^{2+}]_{Free} D_{Ca} + [CaB_1] D_1 + \cdots}{[Ca^{2+}]_{Free} + [CaB_1] + \cdots} = \frac{\sum \kappa_i D_i}{\sum \kappa_i}$$

Results

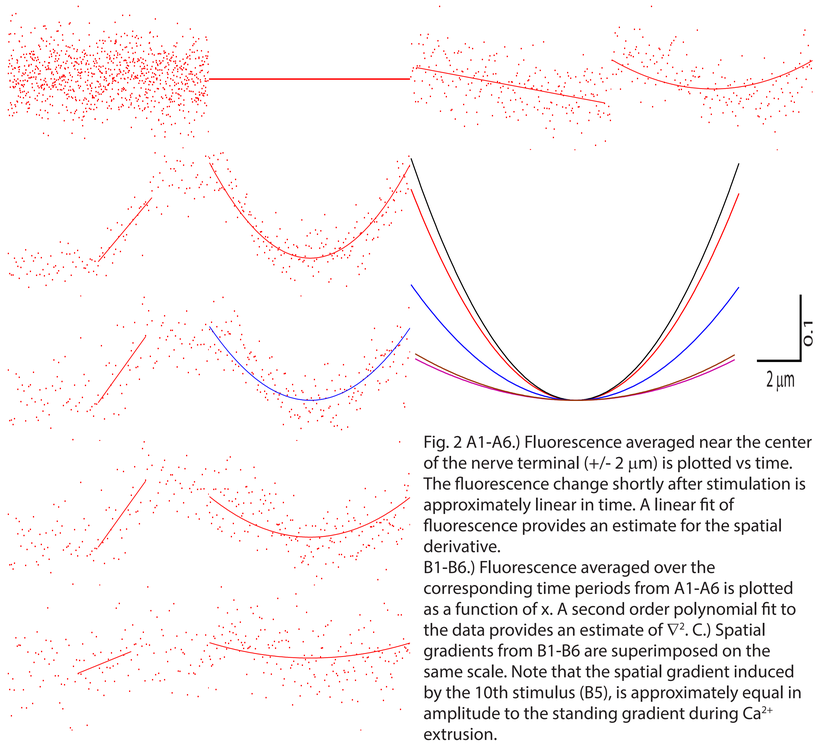

Fig. 2 A1-A6.) Fluorescence averaged near the center of the nerve terminal (+/- 2 μm) is plotted vs time. The fluorescence change shortly after stimulation is approximately linear in time. A linear fit of fluorescence provides an estimate for the spatial derivative.
B1-B6.) Fluorescence averaged over the corresponding time periods from A1-A6 is plotted as a function of x. A second order polynomial fit to the data provides an estimate of ∇^2. C.) Spatial gradients from B1-B6 are superimposed on the same scale. Note that the spatial gradient induced by the 10th stimulus (B5), is approximately equal in amplitude to the standing gradient during Ca^{2+} extrusion.

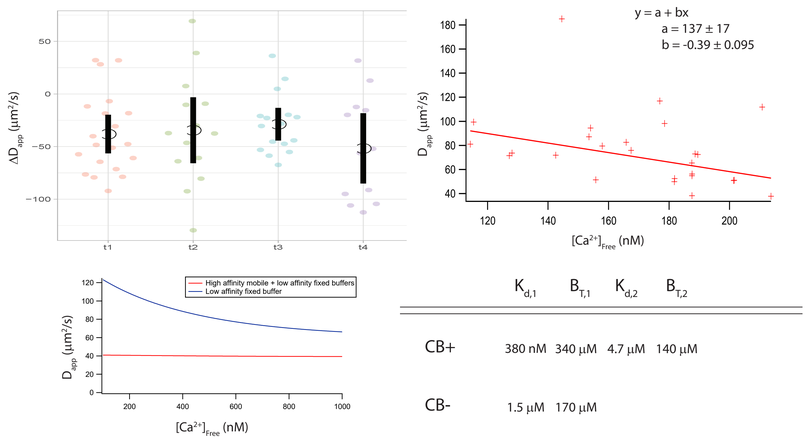

	$K_{d,1}$	$B_{T,1}$	$K_{d,2}$	$B_{T,2}$
CB+	380 nM	340 μM	4.7 μM	140 μM
CB-		1.5 μM	170 μM	

Fig 3. A.) The observed change in D_{app} between the first and second stimulus from sequential trials is plotted for 4 representative nerve terminals (mean and 95% CI indicated in black). Under the null hypothesis that D_{app} is constant $\Delta D_{app} \sim N(0,\sigma^2)$. B.) A linear fit of D_{app} vs $[Ca^{2+}]_{Free}$ suggests a statistically significant relationship. C.) D_{app} vs $[Ca^{2+}]_{Free}$ estimated from eq. 4 for two populations of nerve terminals. D.) Buffering properties for two distinct populations of nerve terminals

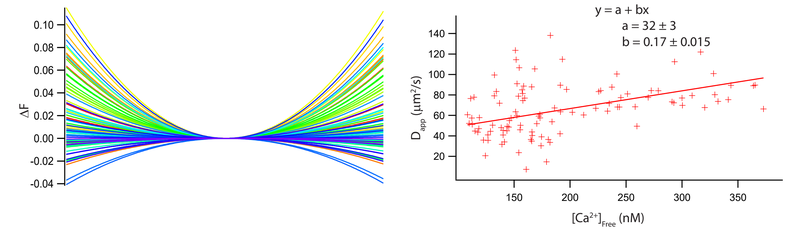

Fig 4. A.) Quadratic fits to spatial profiles 500 ms after the stimulus. F vs T is either flat or decreasing (data not shown), indicating that the Ca^{2+} gradient has collapsed. B.) The fluorescence response to each stimulus was spatially normalized to 250 ms preceeding the stimulus, and analyzed as before., revealing an apparent increase in D_{app} with increasing $[Ca^{2+}]_{Free}$

Discussion

While calcium dynamics play an important role in cellular and synaptic physiology and pathology, Ca^{2+} transport in situ remains poorly explored. Early studies by Allbritton found an anamalously low D_{app} for Ca^{2+} in cytoplasmic extract from xenopus oocytes of 16-65 μm²/s as $[Ca^{2+}]_{Free}$ was increased from 90 nM to 1 μM. Their method of measuring concentrations of Ca^{2+} radioisotopes in frozen sections of extracted cytosol allowed for precise determination of diffusion coefficients at well defined $[Ca^{2+}]_{Free}$. Later work by Neher measured D_{app} in the presence of varying concentrations of Fura-2 in aplysia axons, estimating Dapp ~ 19 μm²/s at zero added Fura-2.
This work represents the first measurements to our knowledge of D_{app} in a mamallian nerve terminal. In the presence of 50 μM Cal-520, we observed Dapp = 123 ± 8 μm²/s during diffusional equilibration in response to a single stimulus delivered to a resting nerve terminal. Repeating the experiments at a series of dye concentrations will allo extrapolation back to an unperturbed nerve terminal.
The second aim of this work is to describe Ca^{2+} transport as a function of $[Ca^{2+}]_{Free}$ to provide additional detail of Ca^{2+} buffering according to eq. 4. However, the analysis was impaired by the formation of an unexplained, stable fluorescence gradient.

Conclusions

1. Buffered calcium diffusion is a concentration dependent process
2. Heterogeneous nerve terminal populations are recapitulated in Ca^{2+} dependence of D_{app}
3. Ca^{2+} dependence of D_{app} provides additional insight into Ca^{2+} buffering processes

Future Directions

1. Estimate D_{app} in unperturbed nerve terminals
2. Estimate D_{app} of biologically neutral substrates such as gold, silver or carbon nanoparticles
3. Correct for induced fluorescence gradient and examine D_{app} as a function of $[Ca^{2+}]_{Free}$

References

McMahon, S. M., Chang, C. W., & Jackson, M. B. (2016). Multiple cytosolic calcium buffers in posterior pituitary nerve terminals. The Journal of general physiology, 147(3), 243-254.
McMahon, S. M., & Jackson, M. B. (2014). In situ Ca2+ titration in the fluorometric study of intracellular Ca2+ binding. Cell calcium, 56(6), 504-512.
Allbritton, N. L., Meyer, T., & Stryer, L. (1992). Range of messenger action of calcium ion and inositol 1, 4, 5-trisphosphate. Science, 258(5089), 1812-1815.
Gabso, M., Neher, E., & Spira, M. E. (1997). Low mobility of the Ca2+ buffers in axons of cultured Aplysia neurons. Neuron, 18(3), 473-481.

Acknowledgments

This work was funded by NIH grant # xxxx